

# Mucosal Region Detection and 3D Reconstruction in Wireless Capsule Endoscopy Videos Using Active Contours

V. B. Surya Prasath<sup>1</sup>, Isabel N. Figueiredo<sup>2</sup>, Pedro N. Figueiredo<sup>3,4</sup>, K. Palaniappan<sup>1</sup>

**Abstract**—Wireless capsule endoscopy (WCE) provides an inner view of the human digestive system. The inner tubular like structure of the intestinal tract consists of two major regions: lumen - intermediate region where the capsule moves, mucosa - membrane lining the lumen cavities. We study the use of the Split Bregman version of the extended active contour model of Chan and Vese for segmenting mucosal regions in WCE videos. Utilizing this segmentation we obtain a 3D reconstruction of the mucosal tissues using a near source perspective shape-from-shading (SfS) technique. Numerical results indicate that the active contour based segmentation provides better segmentations compared to previous methods and in turn gives better 3D reconstructions of mucosal regions.

## I. INTRODUCTION

Wireless capsule endoscopy (WCE) is an expanding imaging modality that is revolutionizing medical diagnostics of the human intestine system [1]. It helps to see inside of the human colon, small bowel and other parts of the digestive system that are normally inaccessible with little or no discomfort to the patient. Usually the captured images (on the order of 50,000 frames) are analyzed by doctors to find anomalies such as bleeding, ulcers, polyps, etc [2], [3], [4]. Recently automatic image processing techniques have been applied to speed up the diagnostic process [5], [6], [7]; see [8] for a recent review. Endoscopic images from WCE provide a circular view of the intestine with mucosa folds and lumen sections, which are two major anatomical constituents of interest. Identification of mucosa folds from each frame of the video is necessary before mucosal based anomalies can be determined. Automated segmentation and labeling greatly facilitates further analysis by enabling physicians to focus on the most diagnostically relevant regions present in WCE video.

A variety of image segmentation techniques exist and a number of methods have been applied to WCE and other endoscopic procedures [9], [10], [11]. Unlike other endoscopic imaging modalities of the intestine, WCE images usually contain multiple folds. Also, gastrointestinal liquids and other materials such as digested food can be present,

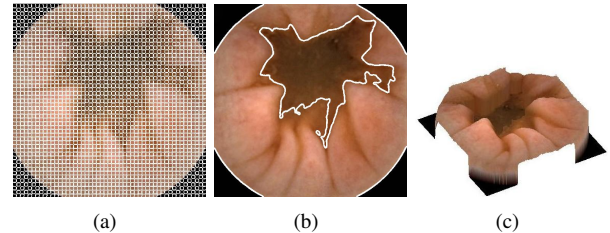


Fig. 1. WCE mucosa segmentation and 3D reconstruction. (a) Input image with the initialization of the fast active contour scheme. (b) Final segmentation curve (at time  $t = 80$ ) laid on top of the original image for visualization. (c) Segmentation based 3D reconstruction of the mucosa part using the shape from shading technique.

see Figure 1 (images obtained by Pillcam<sup>TM</sup> colon capsule, Given Imaging, Yoqneam, Israel). Most of the clustering based segmentation schemes that are based on intensity contrast can fail to identify the mucosa folds properly. The images are non-homogeneous (nonlinear contrast range) in nature, hence thresholding based schemes cannot segment the mucosa folds precisely. In this paper, we report on an approach developed for efficient mucosa detection using a modified variational segmentation scheme based on extending the Chan and Vese active contour without edges model [12] and a 3D reconstruction step using a perspective, near source shape-from-shading (SfS) approach. Perspective and near light source shape from shading models can be studied in a variety of ways [13], [14], [15] and we consider a variational approach which gives robust reconstructions. Numerical results indicate the efficiency of the variational approach for mucosa region segmentation, and further 3D reconstruction results illustrate the potential diagnostic usefulness of our approach.

The rest of the paper is organized as follows. In section II, the active contours without edges method for segmentation and a near-lights perspective SfS scheme are introduced. Section III presents experimental results on a database of WCE videos and Section IV discusses the results and show comparison with other related segmentation schemes.

## II. MUCOSA SEGMENTATION AND 3D RECONSTRUCTION

### A. Active contour based mucosa detection

To avoid the drawbacks of threshold type schemes we make use of the active contour without edges (ACWE) method [12] which gives better segmentation results. Cremers et al [16] extended the ACWE model to include the variance terms for Gaussian distributions of the regions. Suppose that the input image is  $u : \Omega \subset \mathbb{R}^2 \rightarrow \mathbb{R}$ , where

This work was partially supported by the research project UTAustin/MAT/0009/2008 of the UT Austin | Portugal Program (<http://www.utaustinportugal.org/>) and by CMUC and FCT (Portugal), through European program COMPETE/FEDER.

<sup>1</sup>V. B. Surya Prasath K. Palaniappan are with the Department of Computer Science, University of Missouri-Columbia, Columbia MO 65211, USA {prasaths, palaniappan}@missouri.edu

<sup>2</sup>Isabel N. Figueiredo is with the Department of Mathematics, University of Coimbra, Portugal isabel.f@mat.uc.pt

<sup>3,4</sup>Pedro N. Figueiredo is with the Faculty of Medicine, University of Coimbra, Portugal and also with the Department of Gastroenterology, University Hospital of Coimbra, Portugal pnf11@sapo.pt

$\Omega$  represents the image domain. Then the variance extended piecewise constant ACWE is defined by

$$\begin{aligned} \min_{\phi, c_1, c_2} E(\phi, c_1, c_2) &= \alpha \int_{\Omega} |\nabla H(\phi)| dx + \log\left(\frac{\sigma_2}{\sigma_1}\right) \\ &+ \int_{\Omega} \frac{|u - c_1|^2}{2\sigma_1^2} H(\phi) dx + \int_{\Omega} \frac{|u - c_2|^2}{2\sigma_2^2} (1 - H(\phi)) dx \end{aligned} \quad (1)$$

where  $\alpha \geq 0$  is a fixed parameter,  $\sigma_1, \sigma_2$  are the foreground and background region variances,  $c_1, c_2$  represent mean values of regions inside and outside the level set function  $\phi$  respectively. The function  $H(z) := 1$  if  $z \geq 0$ ,  $H(z) := 0$  if  $z < 0$  is the Heaviside function. For solving the above  $L^1$  regularized segmentation problem (1) we make use of the Split-Bregman approach [17] which provides efficient mucosa segmentations, see [18] for a similar approach. More flexible level set methods using multiple phases [19], [20], graph partitioning active contours [21], or edge profile local context [22] can be adapted for improved mucosa segmentation.

### B. Reconstruction of mucosal surface

Due to the nature of the WCE optical system we use a near-light perspective SfS technique for 3D reconstruction  $S$  from the input image  $u$ . Using the mask created from the segmentation  $\{x \in \Omega : \phi(x) < 0\}$  we visualize the surface  $S$  only for captured mucosal regions. We study a near light source SfS model using the following variational minimization approach

$$\begin{aligned} \min_{z, p, q} E(z, p, q) &= \omega \int_{\Omega} (u(x) - R(x, y, z, p, q))^2 dx \\ &+ (1 - \omega) \int_{\Omega} \rho(|\nabla z|, |\nabla p|, |\nabla q|) dx \end{aligned} \quad (2)$$

Here the we assume four near-lights and the reflectance function is given by

$$R = I_0 \sum_{i=1}^4 \left( \frac{\vec{n} \cdot \vec{l}_i}{r_i^3} \right)$$

where  $I_0$  is the light intensity (assumed constant for all lights),  $\vec{n}$  surface normal,  $\vec{l}_i$  light rays incident at point  $(x, y, z)$ ,  $r_i$  the distance of light source  $i$  to the surface and  $\rho$  a robust error function. Following, Wu et al. [15], a gradient descent based discretization is used to obtain the solution of the above minimization and the obtained surface  $S$  provides a 3D visualization of the input image  $u$ . We utilize a single image SfS scheme whereas there are efforts to use neighboring frames via SIFT feature matching technique [23] or elastic registration [24]. We found that for many cases SIFT features are not reliable due to lack of texture in many frames and registration can fail due to abrupt movement of the camera which causes large mucosal surface change between frames.

## III. EXPERIMENTAL RESULTS

The segmentation method is tested on a database consisting 22300 images from 223 short videos (100 frames each) of colon (178, Pillcam COLON1 capsule), small bowel (45, Pillcam SB capsule) taken from 6 patients. The database is collected over a period of one year (2010) at the University Hospital of Coimbra, Portugal. For the Split Bregman algorithm, time step parameter  $\Delta t = 0.5$ , and step size for the finite difference grid  $h = 1$  are fixed for all the videos. The scheme usually converges within  $t = 40$  iterations and the maximum iteration limit is set at  $T = 80$ . The parameters  $w = 0.005$ , and iteration  $T = 20$  of the gradient descent in the SfS scheme (2) are fixed and the time step parameter is adjusted according to the energy decrease. Further we used  $\rho(s_1, s_2, s_2) = \sum_i s_i^2$  for getting smoother surfaces and we are currently exploring other robust functions for getting less smoother reconstructions. In our MATLAB based implementation core algorithms are setup in  $C$  through the *mex* interface and it takes 0.32 seconds per frame ( $512 \times 512$ ) on a Windows7 machine with 2.20GHz, Intel Core2 duo processor. This means the scheme can be used to visualize the segmentations at about 3 frames per second. Although among active contour based schemes the Split Bregman based implementation offers the fastest final segmentation, this running time is still slightly higher than the frame rate of a typical Pillcam colon WCE device. The new Pillcam COLON 2 capsule provides images captured with 4–35 frames per second.

Figure 1 shows an example of the segmentation obtained with the Split Bregman based active contour approach. The original medical image is a typical normal mucosa of the human colon captured in vivo by the WCE device. To obtain a good segmentation we always start with the initialization shown in Figure 1(a). This fine mesh type of initialization has proven to provide better segmentations. Moreover, we observed experimentally that, using a single or seed of coarse circles initializations, the scheme took more iterations to converge. The final segmentation result, in Figure 1(b), shows the mucosal folds and the reconstruction in Figure 1(c) shows a clear boundary between the lumen section.

## IV. DISCUSSION

To compare the efficiency and accuracy of the segmentation scheme (1), we have chosen other related segmentation methods: Otsu type adaptive thresholding technique [11], an image statistics based approach [25], and a globally convex minimization model [26]. Moreover, we benchmark segmentation results of these schemes with expert manual segmentation. As usual in endoscopy image analysis, manual segmentation is considered as gold standard. Visual inspection of the segmentation results in Figure 2 indicate that the active contour based scheme, in general, gives better results than other schemes. Mean shift based scheme (Figure 2(b)) gives a bad result due to the in-homogenous nature of WCE images. Both the Otsu thresholding (Figure 2(a)) and the global minimization scheme (Figure 2(c)) tend to capture the intermediate lumen region, which has high contrast, as

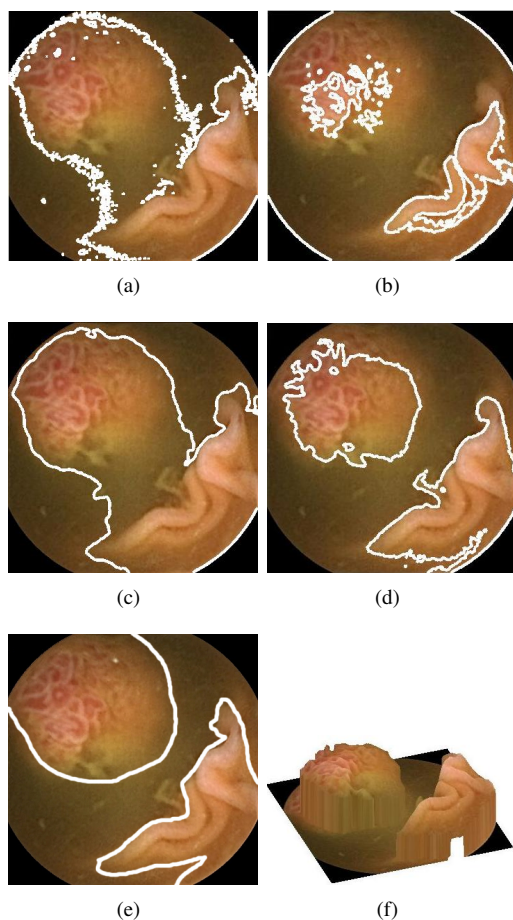


Fig. 2. Comparison of other segmentation schemes with the variational method. (a) Otsu type adaptive thresholding [11]  $\kappa = 0.7388$  (b) Mean-shift [25]  $\kappa = 0.4911$  (c) globally convex minimization [26]  $\kappa = 0.7581$  (d) active contour  $\kappa = 0.7682$  (e) Manual segmentation (used to benchmark the four schemes) (f) Segmented parts shown separately in 3D as surface maps using the segmentation obtained in (d).

opposed to the better segmentation of the ACWE result (Figure 2(d)), when compared to the manual segmentation result in Figure 2(e). The kappa index (also known as Dice coefficient or similarity index) is used to compare the expert-based segmentation with those obtained with the automatic schemes. By definition, for two binary segmentations  $A$  and  $B$ , the kappa index is computed as:

$$\kappa(A, B) = \frac{2|A \cap B|}{|A| + |B|}$$

Here the binary segmentation is computed automatically, using the segmentation curves and by thresholding the regions obtained by the schemes. The notation  $|A|$  denotes the number of pixels in the set  $A$ . Note that, a  $\kappa$  value of 1 indicates perfect agreement. In particular, higher numbers indicate that the results of that particular scheme match the gold standard better than results that produce lower Dice coefficients.

Though this particular segmentation quality metric gives almost equal values for the Otsu thresholding and the global convex minimization segmentation model (see sub-figures 2(a) and (c)), when compared with the manual

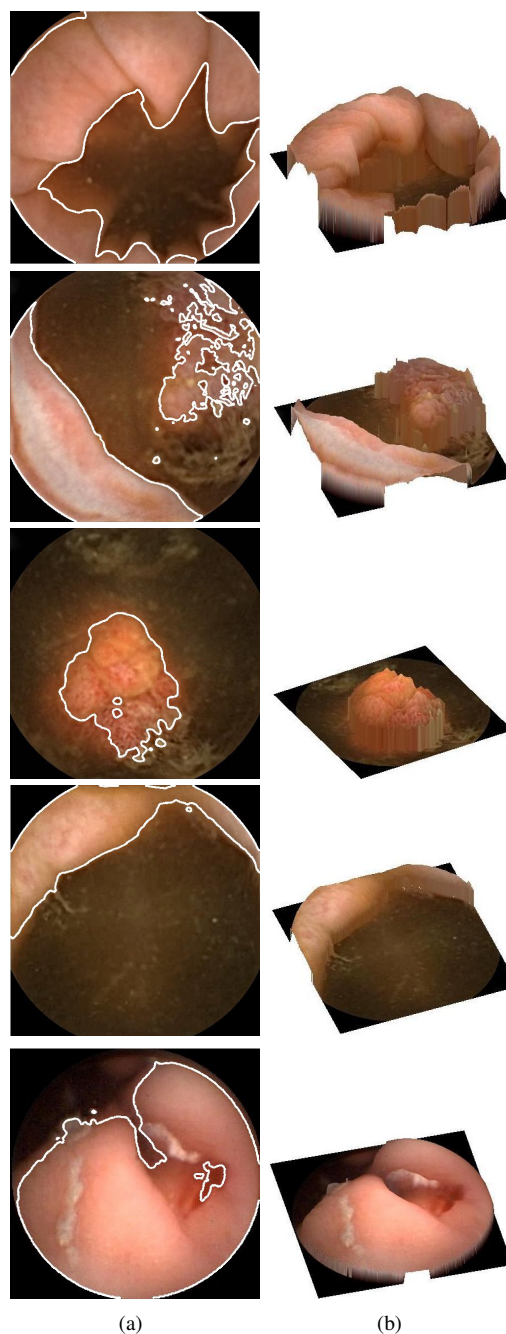


Fig. 3. Examples of frames from colon video mucosa detection and reconstruction. (a) Active contour segmentation with Split Bregman implementation. (b) Segmentation based SfS reconstruction of mucosal regions.

segmentation (Figure 2(e)), the intermediate lumen region is wrongly captured as mucosa. It should be noted that, the aim of the lumen/mucosa regions segmentation is to differentiate the mucosa regions from the lumen section of the intestine. Thus utilizing a better error metric which uses a topological constraint such as [27] for comparison is interesting and defines our future work. By comparing all the four schemes, the active contour method gives better mucosa segmentation, and it clearly separates the two different mucosal regions. The brain-like mucosa in the reconstruction, Figure 2(f) (the top left part) is, in fact, a polyp which is captured by the active contour based scheme.



Finally, Figure 3 shows segmentation and reconstruction results from WCE videos. The frames shown in second and third rows contain a polyp. They are medically significant and detecting them is an important task. The segmentation scheme identifies two regions: the polyp and a non-intersecting mucosal fold and the corresponding 3D reconstruction results 3(b) highlight these regions. Note that, we get a coarse segmentation of the polyp boundary using our scheme and it can further be refined to capture the polyp region alone using other features, such as color or texture. As it can be seen, most of the frames contain trash liquid and other particles, and some have little or no mucosa folds (see fourth row). The last row shows a frame containing a bleeding region from small bowel and the scheme detects the small bleeding region as well.

## V. CONCLUSIONS

We consider a combined lumen and mucosa detection, segmentation and 3D reconstruction scheme for WCE video of the human digestive tract (especially the small bowel and colon). We studied the feasibility of a variance stabilized active contour based segmentation for WCE videos. A perspective, near source SfS technique is used to obtain 3D reconstruction of mucosal regions. Experiments conducted on a database of images and videos from different WCE exams shows the promise of this variational minimization approach for efficient mucosa segmentation and reconstruction. Compared with other segmentation approaches the active contour based method performs reasonably well and gives better mucosa separation with more topologically accurate boundaries. Although the segmentation guided single SfS works fairly well for the WCE images considered here, utilizing the temporal information through the use of neighboring frames to get better 3D reconstructions and using the segmentation area to identify uninformative frames [28] are part of our future direction.

## REFERENCES

- [1] G. Iddan, G. Meron, A. Glukhovsky, and F. Swain, "Wireless capsule endoscopy," *Nature*, vol. 405, no. 6785, pp. 417, 2000.
- [2] R. Eliakim et al, "Evaluation of the pillcam colon capsule in the detection of colonic pathology: results of the first multicenter, prospective, comparative study," *Endoscopy*, vol. 38, no. 10, pp. 963–970, 2006.
- [3] R. Eliakim et al, "Prospective multicenter performance evaluation of the second-generation colon capsule compared with colonoscopy," *Endoscopy*, vol. 41, no. 12, pp. 1026–1031, 2009.
- [4] R. Eliakim, "The pillcam COLON capsule – a promising new tool for the detection of colonic pathologies," *Current Colorectal Cancer Reports*, vol. 4, no. 1, pp. 5–9, 2008.
- [5] I. N. Figueiredo, S. Prasath, Y.-H. R. Tsai, and P. N. Figueiredo, "Automatic detection and segmentation of colonic polyps in wireless capsule images," Tech. Rep. 10–37, University of Coimbra, Portugal, 2010.
- [6] Pedro N. Figueiredo, Isabel N. Figueiredo, Surya Prasath, and Richard Tsai, "Automatic polyp detection in pillcam colon 2 capsule images and videos: Preliminary feasibility report," *Diagnostic and Therapeutic Endoscopy*, vol. 2011, pp. 7pp, 2011, Article ID 182435.
- [7] R. Kumar, Q. Zhao, S. Seshamani, G. Mullin, G. Hager, and T. Dasopoulos, "Assessment of Crohns disease lesions in wireless capsule endoscopy images," *IEEE Transactions on Biomedical Engineering*, vol. 59, no. 2, pp. 355–362, 2012.
- [8] A. Karargyris and N. Bourbakis, "A survey on wireless capsule endoscopy and endoscopic imaging. a survey on various methodologies presented," *IEEE Engineering in Medicine and Biology Magazine*, vol. 29, no. 1, pp. 72–83, 2010.
- [9] M. P. Tjoa, S. M. Krishnan, C. Kugean, P. Wang, and R. Doraiswami, "Segmentation of clinical endoscopic image based on homogeneity and hue," in *23rd IEEE/EMBS International Conference*, 2001, vol. 3, pp. 2665–2668.
- [10] M. P. Tjoa and S. M. Krishnan, "Texture-based quantitative characterization and analysis of colonoscopic images," in *24th IEEE/EMBS International Conference*, 2002, vol. 2, pp. 1090–1091.
- [11] K. Vijayan Asari, "A fast and accurate segmentation technique for the extraction of gastrointestinal lumen from endoscopic images," *Medical Engineering and Physics*, vol. 22, no. 2, pp. 89–96, 2000.
- [12] T. F. Chan and L. A. Vese, "Active contours without edges," *IEEE Transactions on Image Processing*, vol. 10, no. 2, pp. 266–277, 2001.
- [13] A. Tankus, N. Sochen, and Y. Yeshurun, "Shape-from-shading under perspective projection," *International Journal of Computer Vision*, vol. 63, no. 1, pp. 21–43, 2005.
- [14] E. Prados, F. Camilli, and O. Faugeras, "A unifying and rigorous shape from shading method adapted to realistic data and applications," *Journal of Mathematical Imaging and Vision*, vol. 25, no. 3, pp. 307–328, 2006.
- [15] C. Wu, S. G. Narasimhan, and B. Jaramaz, "A multi-image shape-from-shading framework for near-lighting perspective endoscopes," *International Journal of Computer Vision*, vol. 86, no. 2–3, pp. 211–228, 2010.
- [16] D. Cremers, M. Rousson, and R. Deriche, "A review of statistical approaches to level set segmentation: integrating color, texture, motion and shape," *International Journal of Computer Vision*, vol. 72, no. 2, pp. 195–215, 2007.
- [17] T. Goldstein, X. Bresson, and S. Osher, "Geometric applications of the split Bregman method: segmentation and surface reconstruction," *Journal of Scientific Computation*, vol. 45, no. 1–3, pp. 272–293, 2010.
- [18] V. B. Surya Prasath, I. N. Figueiredo, and P. N. Figueiredo, "Colonic mucosa detection in wireless capsule endoscopic images and videos," in *Congress on Numerical Methods in Engineering (CMNE 2011)*, Coimbra, Portugal, June 2011.
- [19] F. Bunyak, A. Hafiane, and K. Palaniappan, "Histopathology tissue segmentation by combining fuzzy clustering with multiphase vector level sets," in *Software Tools and Algorithms for Biological Systems (Eds. H.R. Arabnia and Q.N. Tran)*, vol. 41 of *Advances in Experimental Medicine and Biology*, pp. 413–424. Springer, 2011.
- [20] A. Hafiane, F. Bunyak, and K. Palaniappan, "Fuzzy clustering and active contours for histopathology image segmentation and nuclei detection," in *Advanced Concepts for Intelligent Vision Systems (ACIVS)*, 2008, pp. 903–914, Springer LNCS Volume 5259.
- [21] F. Bunyak and K. Palaniappan, "Efficient segmentation using feature-based graph partitioning active contours," in *12th IEEE International Conference on Computer Vision (ICCV)*, 2009, pp. 873–880.
- [22] I. Ersoy, F. Bunyak, K. Palaniappan, M. Sun, and G. Forgacs, "Cell spreading analysis with directed edge profile-guided level set active contours," in *MICCAI*, 2008, pp. 376–383, Springer LNCS Volume 5241.
- [23] Y. Fan and B. Li M. Q.-H. Meng, "3D reconstruction of wireless capsule endoscopy images," in *32nd IEEE/EMBS International Conference*, 2010, pp. 5149–5152.
- [24] A. Karargyris and N. Bourbakis, "Three-dimensional reconstruction of the digestive wall in capsule endoscopy videos using elastic video interpolation," *IEEE Transactions on Medical Imaging*, vol. 30, no. 4, pp. 957–971, 2011.
- [25] D. Comaniciu and P. Meer, "Mean shift: A robust approach toward feature space analysis," *IEEE Transactions on Pattern Analysis and Machine Intelligence*, vol. 24, no. 5, pp. 603–619, 2002.
- [26] X. Bresson, S. Esedoglu, P. Vanderghenst, J. Thiran, and S. Osher, "Fast global minimization of the active contour/snake model," *Journal of Mathematical Imaging and Vision*, vol. 28, no. 2, pp. 151–167, 2007.
- [27] V. Jain et al, "Boundary learning by optimization with topological constraints," in *IEEE Conference on Computer Vision and Pattern Recognition (CVPR)*, 2010, pp. 2488–2495.
- [28] M. K. Bashar, T. Kitasaka, Y. Suenaga, Y. Mekada, and K. Mori, "Automatic detection of informative frames from wireless capsule endoscopy images," *Medical Image Analysis*, vol. 14, no. 3, pp. 449–470, 2010.